Reverse Engineering of Proteasomal Translocation Rates

D.S. Goldobin,[1,2] M. Mishto,[3,4] K. Textoris-Taube,[4] P.M. Kloetzel,[4] and A. Zaikin[5]

[1] *Department of Physics, University of Potsdam, Postfach 601553, D–14415 Potsdam, Germany*
[2] *Department of Theoretical Physics, Perm State University, 15 Bukireva str., 614990, Perm, Russia*
[3] *CIG, University of Bologna, I–40126 Bologna, Italy*
[4] *Institute of Biochemistry, Charité, Humboldt University, Monbijoustr. 2, 10117 Berlin, Germany*
[5] *Departments of Mathematics and IFWH, University College London, Gower street, WC1E 6BT London, UK*

We address the problem of proteasomal protein translocation and introduce a new stochastic model of the proteasomal digestion (cleavage) of proteins. In this model we account for the protein translocation and the positioning of cleavage sites of a proteasome from first principles. We show by test examples and by processing experimental data that our model allows reconstruction of the translocation and cleavage rates from mass spectroscopy data on digestion patterns and can be used to investigate the properties of transport in different experimental set-ups. Detailed investigation with this model will enable theoretical quantitative prediction of the proteasomal activity.

PACS numbers: 05.40.-a, 87.15.R-, 87.19.xw

arXiv:0804.0682v2 [q-bio.OT] 28 Jul 2008

A macromolecular complex, the proteasome, is the central molecular machine for the degradation of intracellular proteins [1]. Proteasomes have a pivotal role in antigen processing that prepares epitopes for an immune system [2]. They exist in cells as the free proteolytically active core, the barrel-shaped 20S proteasome (Fig. 2b), and as associations of this core with regulatory complexes (PA700 or PA28) at its ends [3]. Here we consider *in vitro* proteasomal digestion assays widely used in molecular biology and immunology to investigate proteasomes.

A protein (Fig. 1) enters the proteasome and is translocated into the central chamber where it is cleaved into fragments by the cleavage sites. We assume that 6 cleavage sites are arranged along two rings (Fig. 2). Fragments of the protein produced are removed through proteasome gates. The translocation proteasomal function can qualitatively change the expression of the specific fragment, *e.g.*, an epitope, because modified translocation and thus increased time of residence near the cleavage terminal changes the conditions of cleavage. Moreover, impairment of proteasomal degradation, probably due to translocation malfunction, might contribute to the pathology of various neurodegenerative conditions [4].

The mechanism of protein translocation remains unknown. It is also unknown whether translocation properties are different for different proteasome types (constitutive or immuno-), with/without different regulatory complexes, and with different experiment conditions (concentration ratios, temperature, *etc.*). Only a few papers address the translocation problem but these are either based on semi-phenomenological descriptions of uptaking and translocation of the protein [5, 6, 7] or they suggest a transport mechanism hypothesis not yet verified experimentaly [8]. On the other hand, there exist several facilities [9, 11] to predict where the protein will be cleaved but as numerous experiments show [12] these algorithms do not always work reliably. The reason is that these algorithms utilize experimental data resulted eventually from some specific protein sequence and translocation function, but the prediction is made based only on the sequence, ignoring the translocation function. In contrast to these approaches, here we introduce a stochastic model which allows one to *reconstruct* both the translocation and cleavage rates from mass spectroscopy (MS) data on digestion patterns. Collecting the reconstructed features of a specific proteasome type can be used for a reliable prediction of the fragment expression.

In our model of protein translocation and degradation by the proteasome we assume that:
(1) The event rate of the protein shift by one amino acid (aa) into the proteasome (to the right in Fig. 2) depends only on the length x of the protein forward end beyond the cleavage sites nearest to the proteasome chamber entrance used for protein infiltration (the left ones in Fig. 2); this event rate is given by the translocation rate function (TRF) $v(x) \equiv v_x$. The backward motions of the entering strand are neglected. These assumptions do not impose significant restrictions on the physical mechanism of the translocation process: they are valid for the Brownian drift in a tilted spatially-periodic potential [10] as well as for the ratchet effect [8], *etc.* The TRFs of different proteasome species (20S, 26S, ±PA28 [3]) may differ.
(2) When the protein strand is close to the cleavage site, the event rate of the cleavage depends on the sequence of aa nearest to the peptide bond cleaved [11]. For the given protein, this conditional cleavage rate (CCR), $\gamma(\tau) \equiv \gamma_\tau$, is a function of the bond number τ (Fig. 1); later on we use τ near the first ring of cleavage sites as a *time-like variable*.
(3) The peptides (cleaved parts of the protein degraded) leave the chamber through proteasome gates. Due to their mobility being higher in comparison to that of the protein, processed peptides leave the chamber quick enough to neglect both their possible further splitting and their influence on the protein transport.

Let us now introduce the distribution $w(x|\tau)$ which is

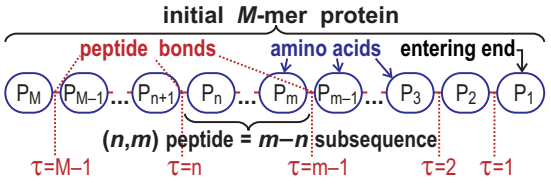


FIG. 1: Peptide bonds are indexed with τ, aa with P_i

the probability of the protein forward end beyond the first ring of the cleavage sites to be of the length x, when the τth bond is near that ring, in our terms, at the discrete "time moment" τ. We measure x in aa, thus x and τ are integer. To describe the "temporal" evolution of distribution $w(x|\tau)$, we consider the shift of the protein strand into the proteasome for one aa, *i.e.*, the transition $\tau \to \tau+1$. Let us decompose $w(x|\tau+1)$ as

$$w(x|\tau+1) = \textstyle\sum_j w_j(x|\tau+1)\,,$$

where $w_j(x|\tau+1)$ are the contributions due to different scenarios of this transition. Along with $w(x|\tau)$, we account $Q(n,m|\tau)$, the amount of the peptide (n,m), which is the m–n subsequence of the degraded protein (Fig. 2), generated during transition $\tau \to \tau+1$.

There are three possible elementary events:
(a) the protein strand shift: $x \to x+1$, $\tau \to \tau+1$; the event rate is v_x;
(b) the cleavage on the first ring of cleavage sites ($x=0$): $x \to 0$, $\tau \to \tau$; the event rate is γ_τ;
(c) the cleavage on the second ring of cleavage sites ($x = L$, L is the distance between the rings of cleavage sites,

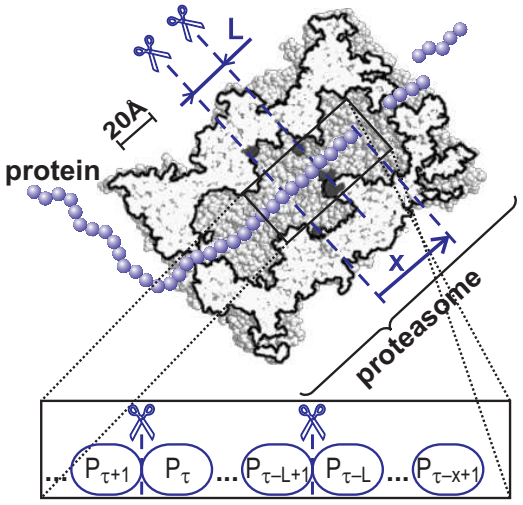


FIG. 2: Infiltration of a protein strand into the 20S proteasome: The scissors mark the positions of cleavage sites rings at $x=0$ and $x=L$; the cleavage occurs via the attaching-detaching of the protein to cleavage sites (dark-grey color); thus, in the figure the bonds between $P_{\tau+1}$ and P_τ and between $P_{\tau-L+1}$ and $P_{\tau-L}$ may be cleaved. The first aa has index $\tau-x+1$ after $\tau-x$ aa have been cut out (see inset).

Fig. 2): $x \to L$, $\tau \to \tau$; the event rate is $\gamma_{\tau-L}$.

In terms of these elementary events the possible scenarios of transition $\tau \to \tau+1$ are
1) *Elementary event (a).* Its probability is

$$P_1(x|\tau) = v_x/\big(v_x+\gamma_\tau+\Theta(x-L-1)\gamma_{\tau-L}\big),$$

where the Heaviside function $\Theta(x<0)=0$, $\Theta(x\geq 0)=1$. In this scenario, $x \to x+1$, and

$$w_1(x+1|\tau+1) = P_1(x|\tau)\,w(x|\tau)\,. \qquad (1)$$

No peptides are generated;
2) *Elementary event (b)*, which may not be followed by anything but the strand shift by one aa (as there is nothing to be cleaved). This scenario probability is

$$P_2(x|\tau) = \gamma_\tau/\big(v_x+\gamma_\tau+\Theta(x-L-1)\gamma_{\tau-L}\big).$$

In this scenario, $x \to 1$, and

$$w_2(x|\tau+1) = \delta_{x,1}\textstyle\sum_{x'=1}^{\infty} P_2(x'|\tau)\,w(x'|\tau)\,. \qquad (2)$$

The peptides cut out are

$$Q_2(\tau,\tau-x+1|\tau) = P_2(x|\tau)\,w(x|\tau)\,; \qquad (3)$$

3) *Elementary event (c), which may be followed either by strand shift (1) or by scenario (2).* The probability of the first stage (c) is

$$P_c(x|\tau) = \Theta(x-L-1)\,\gamma_{\tau-L}/\big(v_x+\gamma_\tau+\gamma_{\tau-L}\big).$$

After event (c), when $x \to L$, the number of the system states generated is

$$w_c(x|\tau) = \delta_{x,L}\textstyle\sum_{x'=L+1}^{\infty} P_c(x'|\tau)\,w(x'|\tau)\,,$$

and the peptides cut out are

$$Q_c(\tau-L,\tau-x+1|\tau) = P_c(x|\tau)\,w(x|\tau)\,.$$

The subsequent events (1) or (2) should be regarded as the respective above mentioned scenarios starting with distribution $w_c(x|\tau)$, *i.e.*,

$$\begin{aligned} w_{c1}(x|\tau+1) &= P_1(L|\tau)\,w_c(x-1|\tau) \\ &= P_1(L|\tau)\,\delta_{x,L+1}\textstyle\sum_{x'=L+1}^{\infty} P_c(x'|\tau)\,w(x'|\tau)\,, \qquad (4) \end{aligned}$$

$$\begin{aligned} Q_{c1}(\tau-L,\tau-x+1|\tau) &= P_1(L|\tau)\,Q_c(\tau-L,\tau-x+1|\tau) \\ &= P_1(L|\tau)\,P_c(x|\tau)\,w(x|\tau)\,, \qquad (5) \end{aligned}$$

$$\begin{aligned} w_{c2}(x|\tau+1) &= \delta_{x,1}\textstyle\sum_{x'=1}^{\infty} P_2(x'|\tau)\,w_c(x'|\tau) \\ &= \delta_{x,1}\,P_2(L|\tau)\textstyle\sum_{x'=L+1}^{\infty} P_c(x'|\tau)\,w(x'|\tau)\,, \qquad (6) \end{aligned}$$

$$\begin{aligned} Q_{c2}(\tau-L,\tau-x+1|\tau) &= P_2(L|\tau)\,Q_c(\tau-L,\tau-x+1|\tau) \\ &= P_2(L|\tau)\,P_c(x|\tau)\,w(x|\tau)\,. \qquad (7) \end{aligned}$$

$$\begin{aligned} Q_{c2}(\tau,\tau-x+1|\tau) &= P_2(x|\tau)\,w_c(x|\tau) \\ &= \delta_{x,L}\,P_2(L|\tau)\textstyle\sum_{x'=L+1}^{\infty} P_c(x'|\tau)\,w(x'|\tau)\,. \qquad (8) \end{aligned}$$

Collecting Eqs. (1),(2),(4),(6), we find master equation

$$w(1|\tau+1) = \sum_{x=1}^{L} \frac{\gamma_\tau\, w(x|\tau)}{v_x+\gamma_\tau} + \sum_{x=L+1}^{\infty} \frac{\gamma_\tau\, w(x|\tau)}{v_x+\gamma_\tau+\gamma_{\tau-L}} + \frac{\gamma_\tau}{v_L+\gamma_\tau} \sum_{x=L+1}^{\infty} \frac{\gamma_{\tau-L}\, w(x|\tau)}{v_x+\gamma_\tau+\gamma_{\tau-L}}; \quad (9)$$

$$w(L+1|\tau+1) = \frac{v_L}{v_L+\gamma_\tau} \times \left[w(L|\tau) + \sum_{x=L+1}^{\infty} \frac{\gamma_{\tau-L}\, w(x|\tau)}{v_x+\gamma_\tau+\gamma_{\tau-L}} \right]; \quad (10)$$

$x \neq 1,\ x \neq L+1$:

$$w(x|\tau+1) = \frac{v_{x-1}\, w(x-1|\tau)}{v_{x-1}+\gamma_\tau+\Theta(x-L-1)\gamma_{\tau-L}}. \quad (11)$$

Here $x = 1, 2, 3, ..., M$ and $\tau = 1, 2, 3, ..., M-1$, where M is the length of the protein (Fig. 2).

Performing numerical simulation of degradation of Mmer polypeptide, one should start at $\tau = 1$ with $w(x|\tau = 1) = \delta_{x,1}$ and iterate Eqs. (9)–(11) till the last $\tau = M-1$. Additionally, the releasing of the last fragment from the chamber at the "time moment" $\tau = M$ should be taken into account: $Q(M, M-x+1|M) \to Q(M, M-x+1|M) + w(x|M)$. Hence, with $w(x|\tau)$ known for $\tau = 1, 2, ..., M$, one can summarize Eqs. (3), (5), (7) and (8) for to evaluate the digestion pattern, *i.e.* the total amount $Q(m,n)$ of the peptide (n,m) generated during a single polypeptide processing,

$$\begin{aligned} Q(\tau_1,\tau_2) &= Q(\tau_1,\tau_2|\tau_1) + \Theta(M-\tau_1-L)\, Q(\tau_1,\tau_2|\tau_1+L) \\ &= \delta_{\tau_1,M} w(\tau_1+L-\tau_2+1|M) \\ &+ \frac{\gamma_{\tau_1}\, w(\tau_1-\tau_2+1|\tau_1)}{v_{\tau_1-\tau_2+1}+\gamma_{\tau_1}+\Theta(\tau_1-\tau_2-L)\gamma_{\tau_1-L}} \\ &+ \frac{\delta_{\tau_1-\tau_2+1,L}\,\gamma_{\tau_1}}{v_L+\gamma_{\tau_1}} \sum_{x=L+1}^{M} \frac{\gamma_{\tau_1-L}\, w(x|\tau_1)}{v_x+\gamma_{\tau_1}+\gamma_{\tau_1-L}} \\ &+ \Theta(M-\tau_1-L) \frac{\gamma_{\tau_1}\, w(\tau_1+L-\tau_2+1|\tau_1+L)}{v_{\tau_1+L-\tau_2+1}+\gamma_{\tau_1+L}+\gamma_{\tau_1}}, \end{aligned} \quad (12)$$

here $1 \le \tau_2 \le \tau_1 \le M$. Since the protein can be cleaved starting both from the C- and from the N-terminal, the final digestion pattern is given by

$$Q_{\rm fin}(\tau_1,\tau_2) = P_{\rm N}\, Q_{\rm N}(\tau_1,\tau_2) + P_{\rm C}\, Q_{\rm C}(M-\tau_2+1, M-\tau_1+1)\,. \quad (13)$$

The subscripts indicate which terminal goes first, $P_{\rm N}$ and $P_{\rm C} = 1 - P_{\rm N}$ are the probabilities of the degradation starting from the corresponding end.

Digestion pattern $Q_{\rm fin}(\tau_1,\tau_2)$ is a functional of TRF v_x and CCR γ_τ. Utilizing MS data on the digestion pattern, one can determine nonzero values of γ_τ (*i.e.* positions of possible cleavage) and minimize the mismatch between $Q_{\rm fin}(\tau_1,\tau_2)$ and MS data $\widetilde{Q}(\tau_1,\tau_2)$ over v_x, the nonzero values of γ_τ, and $P_{\rm N}$ in order to *reconstruct* them. Note, v_x and γ_τ are defined up to the constant multiplier, which should be determined from the degradation rate in real time, but not from the digestion pattern.

In order to verify the robustness of the reverse engineering procedure, numerous tests have been performed. A typical test presented in Figs. 3a–c has been performed as follows. For given v_x and γ_τ the digestion pattern $Q(\tau_1,\tau_2)$ has been evaluated. The result has been perturbed by noise; $\widetilde{Q}(\tau_1\tau_2) = Q(\tau_1\tau_2) +$

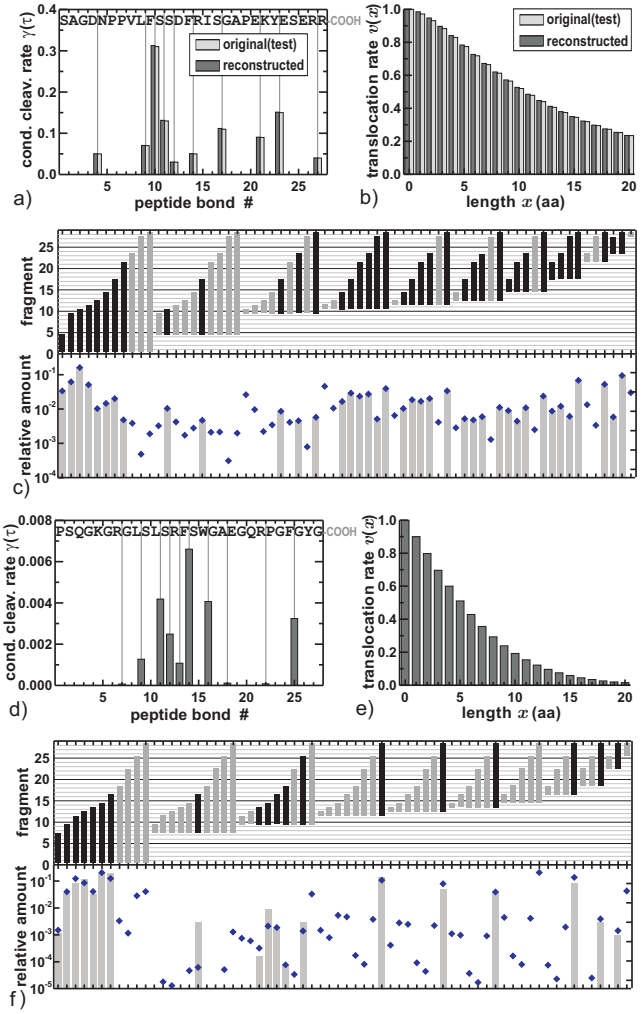


FIG. 3: Test (a–c): Reconstruction of translocation function v_x and conditional cleavage rates γ_τ for the 28mer peptide Kloe 320 [12]. a) the conditional cleavage probabilities and the aa sequence; b) the translocation rate function; c) the upper plot presents a set of digestion fragments (black bars: fragments utilized for the reconstruction, gray bars: not utilized), and the lower plot presents the amount of the corresponding fragment (diamonds: the reconstructed values $Q_{\rm fin}$, gray bars: the values of $\widetilde{Q}$ utilized for the reconstruction). Experiment (d–f): Reconstruction of v_x and γ_τ for the 28mer peptide Kloe 258 degraded by 20S proteasome; $P_{\rm N} = 54\%$.

$10^{-4} R_{\tau_1,\tau_2}\sqrt{Q(\tau_1,\tau_2)}$, where R_{τ_1,τ_2} are independent random numbers uniformly distributed in $[-1,1]$. The information about 1mer and 2mer fragments and fragments which relative amount is less than $5\cdot10^{-3}$ has been omitted as being hardly acquirable in experiments [13]. Resulting $\widetilde{Q}_{\tau_1\tau_2}$ has been used for the reconstruction of v_x and γ_τ. The original and reconstructed data for γ_τ (Fig. 3a) and v_x (Fig. 3b) are in a good agreement. The reconstructed $P_{\rm N} = 0.49$ against the original $P_{\rm N} = 0.50$.

Figs. 3d–f present the results of the reverse engineering from the experimental (*in vitro*) digestion pattern for the 28mer Kloe 258, which is the sequence 101–128 aa of human Myelin Basic Protein, degraded by 20S proteasomes purified from lymphoblastoid cell lines, which express mainly the immunoproteasome (for materials and methods see [12]). The TRF v_x appears to be monotonically decaying; the reconstructed probability of the degradation starting from the N-terminal $P_{\rm N} = 54\%$, meaning the degradations from the N- and C-ends are almost equally probable in this case.

The suggested reconstruction method has some limitations. The reconstruction procedure for short polypeptides is very sensitive to measurement inaccuracy. Though the whole information on $Q(\tau_1,\tau_2)$ is not needed, the number of nonzero values of $Q(\tau_1,\tau_2)$ utilized for a reliable (tolerant to noise) reconstruction should considerably exceed the number of reconstructed parameters. For Kloe 258 the number of trustworthy and utilized values of $\widetilde{Q}(\tau_1,\tau_2)$ is 19 (see Fig. 3f), it is a bit greater than the number of unknown parameters which is 14. Hence, more accurate and comprehensive MS data on the digestion pattern are needed. Additionally, for short polypeptides the finishing stage of the degradation is relatively important, because on this stage the translocation rate is affected by the edge effects (the backward end of the polypeptide gets inside the proteasome chamber) and is not the same as for the remainder of the polypeptide.

Fast and effective design of new intelligent drugs against immune and autoimmune deceases [2] is impossible without development of the virtual immune system, by which these drugs can be tested *in silico*. One of the most important steps on this road is the prediction of presentation profile, *i.e.* number of epitopes, from transcription to presentation on MHC class I complex and potentially recognized by CD8+ T-cells. To do this, one should be able to predict reliably the proteasomal digestion pattern (DP) that is determined by sequence-specific cleavage preferences (SSCP), that is quantified by CCR in our approach, and proteasomal TRF. Some attempts to fulfill these predictions have been made based on finding the correlations between SSCP and final DP. These algorithms are available on the Internet [9, 11] however they are not always reliable because of ignoring the dependence of DP on TRF. The significance of the mathematical method presented here is the possibility to find dependencies between SSCP, TRF and DP. Using this method and applying it to various experimental data one would be able to construct algorithms for a reliable prediction of proteasomal DP.

In summary, we have proposed a model of the degradation of proteins by the proteasome which allows one to *reconstruct* the proteasomal transport function and cleavage strengthes. The model is applicable to a broad variety of hypothetically possible translocation mechanisms [8, 10]. We have tested the model for relatively short (25–50mers) synthetic polypeptides as the most common case for *in vitro* experiments. Earlier, in [15], we have described how peculiarities of the translocation function may lead to the multimodality of the fragment length distribution even for $\gamma(\tau) \equiv const$. Here we have shown that the amount of each digestion fragment is not only determined by the cleavage map of the substrate but is also crucially affected by nonuniformity of the translocation rate. The proposed methodology can be used in extensive analysis of already available MS data for the 20S proteasomes and its associations with different regulatory complexes and under different experimental conditions. The results of this analysis, specifically, the shape of the translocation rate function and its variations for diverse proteasome species under different conditions, can give insight into the mystery of the protein translocation mechanism inside the proteasome. Such an analysis can elucidate also the unanswered question whether there is some preference for starting the degradation with the N- or C-terminal of the protein, and how this preference is quantitatively affected by regulatory complexes.

We thank S. Witt for fruitful discussions and the VW-Stiftung, PROTEOMAGE (FP6), the BRHE program, and "Perm Hydrodynamics" for financial support.

[1] K. L. Rock *et al.*, Cell **78**, 761 (1994).
[2] P. M. Kloetzel, Nat. Rev. Mol. Cell. Biol. **2**, 179 (2001).
[3] N. Tanahashi *et al*, J. Biol. Chem. **275**, 14336 (2000).
[4] D. C. Rubinsztein, Nature **443**, 780 (2006); M. Mishto *et al.*, CNSA-MC **7**, 236 (2007).
[5] H. G. Holzhütter and P. M. Kloetzel, Biophys. J. **79**, 1196 (2000).
[6] B. Peters *et al.*, J. Mol. Biol. **318**, 847 (2002).
[7] F. Luciani *et al.*, Biophys. J. **88**, 2422 (2005).
[8] A. Zaikin and T. Pöschel, Europhys. Lett. **69**, 725 (2005).
[9] C. Kuttler *et al.*, J. Mol. Biol. **298**, 417 (2000); C. Kesmir *et al.*, Protein Eng. **15**, 287 (2002).
[10] P. Reimann *et al.*, Phys. Rev. Lett. **87**, 010602 (2001).
[11] S. Tenzer *et al.*, Cell. Mol. Life Sci. **62**, 1025 (2005).
[12] M. Mishto *et al.*, J. Mol. Biol. **377**, 1607 (2008); M. Mishto *et al.*, Biol. Chem. **387**, 417 (2006).
[13] A. Kohler *et al.*, Mol. Cell. **7**, 1143 (2001).
[14] A. K. Nussbaum *et al.*, Immunogenetics **53**, 87 (2001).
[15] A. Zaikin *et al.*, Biophys. Rev. Lett. **1**, 375 (2006).